Fig. 17.　Radiation pattern for eight-element array of TMSA shown in Fig. 6, of $\alpha = 75°$, four turns, $L = 5$ mm and $d = 0.5$ mm at an operating frequency of 10 GHz: (a) geometry, (b) $x - z$ plane, (c) $y - z$ plane, and (d) $x - y$ plane.

## IV. CONCLUSION

A new design of a dual tapered meander slot antenna (TMSA) is presented, operating with a center frequency of 10 GHz and bandwidth of about 20%. The TMSA gave a directivity of 4.2 dB and gain of 3 dB as well as a stable radiation pattern across the bandwidth of operation. Cross polarization levels of about $-12$ dB was also observed for eight-element array of this antenna. Verification of the simulation results is verified with measurements for a simpler design. Future research will include the measurements for the final design in an array environment.

## REFERENCES

[1] B. Rulf and G. A. Robertshaw, *Understanding Antennas for Radar, Communications, and Avionics*.　New York: Van Nostrand Reinhold, 1987.
[2] C. P. Wen, "Coplanar waveguide: a surface strip transmission line suitable for nonreciprocal gyromagnetic device applications," *IEEE Trans. Microwave Theory Tech.*, vol. 17, no. 12, pp. 1087–1090, Dec. 1969.
[3] R. C. Hansen, *Phased Array Antennas*.　New York: Wiley, 1998, pp. 1–6.
[4] Agilent Technologies, Advance Design Systems 1.5 Momentum, Dec. 2000.
[5] S.-H. Wi, J.-M. Kim, T.-H. Yoo, H.-J. Lee, J.-Y. Park, J.-G. Yook, and H.-K. Park, "Bow-tie-shaped meander slot antenna for 5 GHz application," in *Proc. APS-URSI Symp.*, vol. 2, San Antonio, TX, Jun. 2002, pp. 456–459.
[6] J.-M. Kim, J.-G. Yook, W.-Y. Song, Y.-J. Yoon, J.-Y. Park, and H.-K. Park, "Compact meander-type slot antennas," in *Proc. APS-URSI Symp.*, vol. 2, Boston, MA, Jul. 2001, pp. 724–727.
[7] C.-K. Wu, K.-L. Wong, and W.-S. Chen, "Slot-coupled meandered microstrip antenna for compact dual-frequency operation," *Electron Lett.*, vol. 34, no. 11, pp. 1047–1048, 1998.
[8] J.-H. Lu and K.-L. Wong, "Slot-loaded, meandered rectangular microstrip antenna with compact dual frequency operation," *Electron Lett.*, vol. 34, no. 11, pp. 1048–1050, 1998.

# On the Wheeler Cap Measurement of the Efficiency of Microstrip Antennas

Hosung Choo, Robert Rogers, and Hao Ling

*Abstract*—The Wheeler cap method for measuring the efficiency of microstrip antennas is revisited. First, we show that the parallel *RLC* model is a more appropriate model to use than a series one for the microstrip antennas under consideration. Our results are verified by numerical simulation using ENSEMBLE. Second, the role of the interior cavity modes is investigated and a reduced-height Wheeler cap is proposed. Finally, the Wheeler cap method is applied to measure the efficiency of miniaturized microstrip antennas designed using genetic algorithms.

*Index Terms*—Antenna efficiency, efficiency measurement, microstrip antennas, Wheeler cap.

## I. INTRODUCTION

The Wheeler cap method is a simple and well-known technique for measuring antenna efficiency [1]–[4]. The method involves making only two input impedance measurements of the antenna under test: one with a conducting cap enclosing the antenna and one without. The antenna efficiency is then estimated based on either a parallel or a series *RLC* circuit model for the antenna. Pozar and Kaufman reported on the use of this method for measuring the efficiency of microstrip antennas [5]. Even though it is generally believed that a microstrip antenna is more appropriately modeled as a parallel circuit [6]–[8], their measurement results did not support the parallel *RLC* model, and they concluded that the loss mechanism in the microstrip antenna is similar to that of a series *RLC* circuit. More recent reports of microstrip antenna efficiency also appear to use the series *RLC* model [9].

In this work, we revisit the Wheeler cap method for measuring the efficiency of microstrip antennas. Our main interest stems from the need to characterize the efficiency of a class of miniaturized microstrip antennas we designed using genetic algorithms (GA) [10]. We report here three main findings. First, we show that the parallel *RLC* model is a more appropriate model to use than the series model for a single-resonance, probe-fed microstrip antenna on a thin substrate. Our measurement results on both FR-4 and RT Duroid substrates are corroborated by numerical simulations using the commercial software ENSEMBLE [11]. Second, we investigate the role of interior cavity modes and propose a reduced-height Wheeler cap for microstrip antennas. Finally,

we apply the Wheeler cap method to investigate the efficiency of our GA-designed miniaturized microstrip antennas.

## II. ANTENNA EQUIVALENT CIRCUIT MODEL

In the Wheeler cap method, two input impedance measurements are needed to obtain the efficiency of an antenna. One is the input impedance before using the cap, and the other is the input impedance after putting the cap on. If the test antenna behaves more like a series $RLC$ circuit near its resonance, then the input resistance $R$ should decrease after applying the cap, and the efficiency is calculated by the following expression:

$$\text{Eff} = \frac{P_R}{P_R + P_L} = \frac{R_R}{R_R + R_L} = \frac{R_{\text{no\_cap}} - R_{\text{cap}}}{R_{\text{no\_cap}}} \tag{1}$$

where $P_R$ is the total radiated power, $P_L$ is the power loss in the antenna structure, $R_R$ is the radiation resistance and $R_L$ is the loss resistance. If the test antenna behaves more like a parallel $RLC$ circuit near its resonance, the efficiency is more appropriately defined in terms of the input conductance $G$ using

$$\text{Eff} = \frac{P_R}{P_R + P_L} = \frac{G_R}{G_R + G_L} = \frac{G_{\text{no\_cap}} - G_{\text{cap}}}{G_{\text{no\_cap}}}. \tag{2}$$

Note that for an antenna represented by the parallel circuit model, $G$ at the antenna resonance should decrease after the cap is placed over the antenna. Therefore, the input resistance $R$ should *increase* after applying the cap, contrary to the series circuit model.

As a test, we apply the Wheeler cap method to measure a standard square-shaped microstrip antenna built on lossy FR-4 substrate of size 87 mm × 87 mm and thickness 1.6 mm. The dimensions of the copper patch of the test antenna are 36 mm × 36 mm, resulting in a resonant frequency of 2 GHz. For the Wheeler cap, we use a conducting rectangular cap ($100$ mm × $50$ mm × $100$ mm) to completely enclose the test microstrip antenna. Then an HP 8753C network analyzer is used to measure the input impedance of the test antenna. As stated in [2], [5], a good contact between the cap and the ground plane is critical for an accurate measurement and aluminum tape is used to ensure a good contact. Fig. 1(a) shows the resulting input resistances before and after applying the cap, shown as a dashed line and a solid line, respectively. At the resonant frequency, it shows $R_{\text{no\_cap}}$ of 65 ohms and $R_{\text{cap}}$ of 113 ohms. Clearly this supports the parallel $RLC$ circuit model as the input resistance increases after the cap is placed. Based on the parallel $RLC$ model, the efficiency is found to be 34% at the resonant frequency.

Next, we verify the measurement result with two different numerical simulations using ENSEMBLE. In the first simulation, we model the Wheeler cap structure to predict $R_{\text{no\_cap}}$ and $R_{\text{cap}}$. The rectangular cavity option in ENSEMBLE is used to model the Wheeler cap (FR-4 dielectric constant 4.1 and loss tangent 0.025, copper conductivity $5.7 \times 10^7$ S/m). The simulated input resistances are shown in Fig. 1(b). Good agreement with Fig. 1(a) is apparent. Based on the parallel circuit model, we compute the efficiency from the simulation data to be 41% at the resonant frequency. In the second simulation, we compute the gain of the test antenna with and without dielectric and metal losses (on the patch and the ground plane). The efficiency is then calculated by taking the ratio $(\text{Gain}_{\text{with-loss}})/(\text{Gain}_{\text{without-loss}})$. The value is found to be 32% at the resonant frequency.

The comparison of the two simulations and the measurement over a range of frequencies is shown in Fig. 2(a). It shows that the two simulation results (the dashed and dash-dotted lines) are within 10% of each other over the $-10$ dB bandwidth around the antenna resonance, and the measurement result (the solid line) falls within this range. As a test, we also try to obtain the efficiency from the measurement data using the series $RLC$ model and the results are plotted in the same figure as
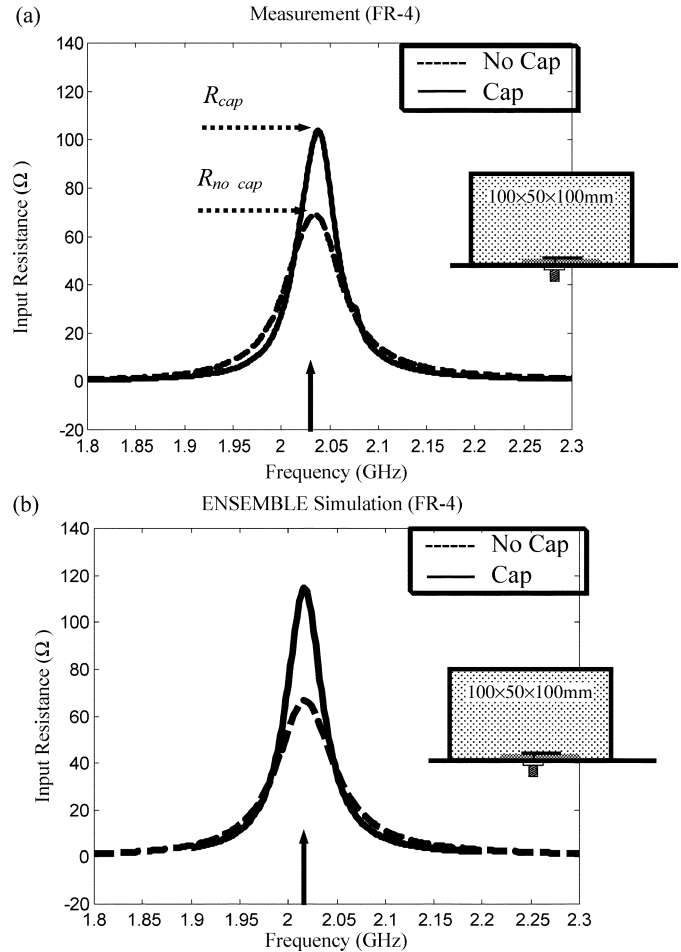


Fig. 1. Input resistance of a standard square-shaped microstrip antenna (36 mm × 36 mm) built on FR-4 substrate before ($-----$) and after ($\underline{\hspace{1.5cm}}$) applying a Wheeler cap of size 100 mm × 50 mm × 100 mm. (a) Measured. (b) ENSEMBLE simulated.

dots. The answer is totally unreasonable, falling mostly below zero in the resonant range. We note that McKinzie [4] proposed an improved method that incorporates an additional transmission line section in the antenna model. By adjusting the phase angle of the transmission line to better match the measured data, it provides a fine adjustment to extract the efficiency from the Wheeler cap measurements. We tried this method on our data and the resulting efficiency changed only slightly, from 34% to 33%.

The same procedure is applied to a microstrip antenna built on a low-loss RT Duroid 5880 substrate of size 45 mm × 45 mm and thickness 1.6 mm. This test microstrip antenna has patch dimensions of 17.5 mm × 24 mm and operates at around 5.3 GHz. The dimensions of the Wheeler cap used in this case are $50$ mm × $50$ mm × $50$ mm. The measurement results are compared against the two simulations over a range of frequencies in Fig. 2(b). Again, good agreement among the three results within the $-10$ dB bandwidth is observed. The efficiency at resonance is found to be 94% by the Wheeler cap measurement, 98% by the Wheeler cap simulation, and 99% by the gain simulation. Also plotted in the figure is the efficiency derived from the measurement data using the series $RLC$ model. Again the series model results look totally unreasonable. This confirms the validity of the parallel $RLC$ model for the microstrip antennas under consideration in Wheeler cap measurements. Furthermore, we observe a frequency dip in both the Wheeler cap measurement and the Wheeler cap simulation in Fig. 2(b) at around 5.12 GHz, which is caused by the excitation of the cavity mode $TM_{111}$
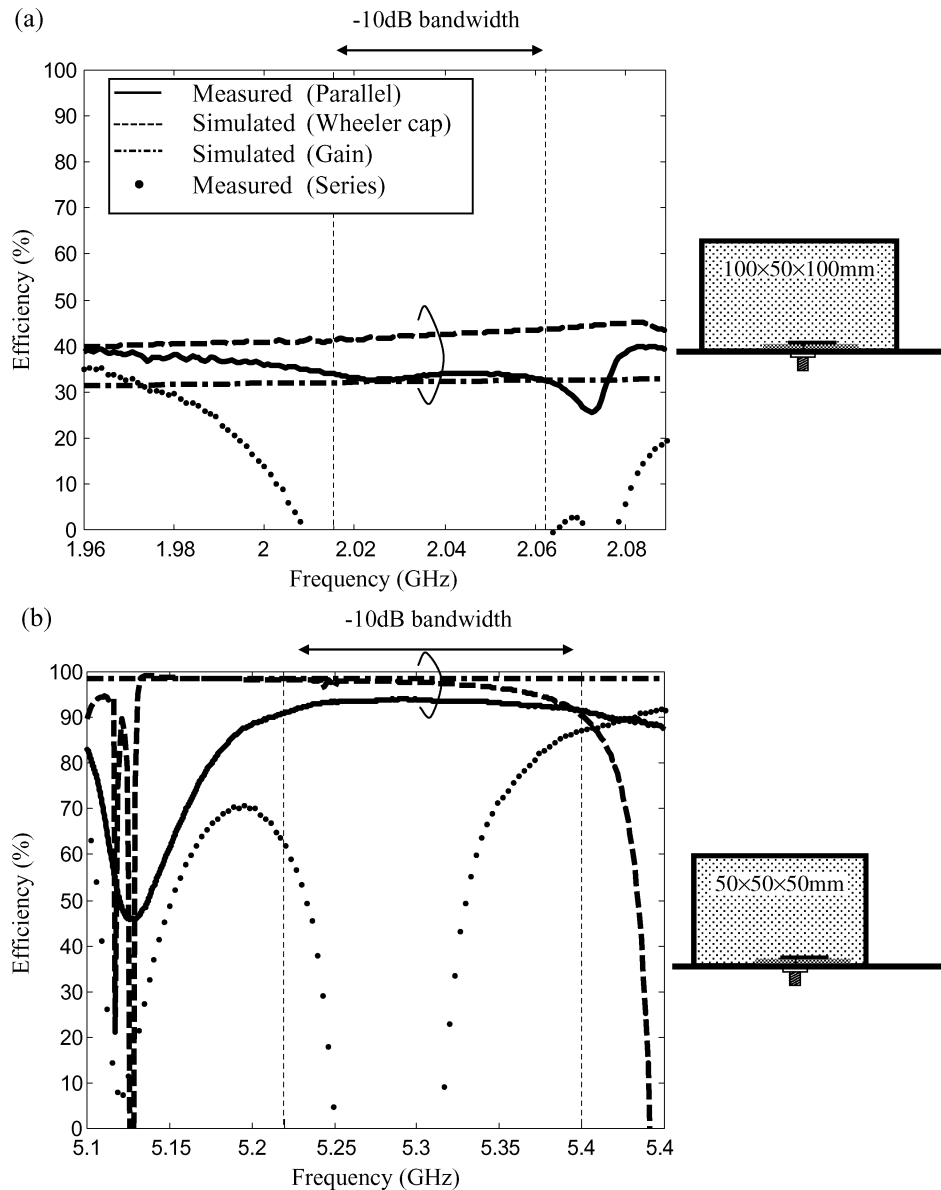
Fig. 2. Measured Wheeler cap efficiency based on parallel circuit model (———), Wheeler cap simulation (— — — — —), gain simulation (—·—·—·—) and efficiency based on series circuit model (●). (a) Microstrip antenna (36 mm × 36 mm) built on FR-4 substrate using a Wheeler cap size of 100 mm × 50 mm × 100 mm. (b) Microstrip antenna (17.5 mm × 24 mm) built on Duroid using a Wheeler cap size of 50 mm × 50 mm × 50 mm.

in the cap. In the next section, we will discuss the effect of cavity modes on efficiency measurements.

## III. EFFECT OF CAP DIMENSIONS

In [1], Wheeler recommended that the cap radius of a spherical cap be around 1/6 of a wavelength to minimize the influence of the cap on the current distribution on the antenna. For microstrip antennas, however, a considerably larger Wheeler cap is often needed to enclose an extended substrate or in some cases a microstrip patch array. Larger Wheeler caps support interior cavity modes that may interfere with the resonant frequency of the microstrip patch to cause a deviation in the input resistance value. This in turn can cause an inaccurate efficiency measurement. For example, the same microstrip patch used in Fig. 2(b) is used again in Fig. 3(a), except with a larger Duroid substrate of dimensions 154 mm × 154 mm. To fully enclose the antenna, a cap size of 170 mm × 85 mm × 170 mm is used. We observe many cavity modes

around the resonant frequency and the microstrip patch resonance is not very prominent.

Thus, we want to make the interior cavity modes as sparse as possible to minimize their influence on the antenna. A detailed look at the interior cavity modes for a rectangular shaped Wheeler cap shows that only TM modes are dominant since the microstrip antenna operates like a horizontal magnetic current parallel to the ground plane. The resonant frequencies are given by [12]

$$ f_{MNP}^{\mathrm{TM}} = \frac{1}{2\pi\sqrt{\mu_0\varepsilon_0}} \sqrt{\left(\frac{M\pi}{a}\right)^2 + \left(\frac{N\pi}{b}\right)^2 + \left(\frac{P\pi}{c}\right)^2}. \quad (3) $$

The second index $N$ is associated with the cap height while the other indexes $M$ and $P$ are associated with the length and the width of the cap, respectively. Fig. 4(a) shows the interior cavity mode spectrum for a Wheeler cap size of 170 mm × 85 mm × 170 mm. The dashed lines show all the permissible modes calculated using (3) while the solid line is the measured input resistance. The peaks in the measured input
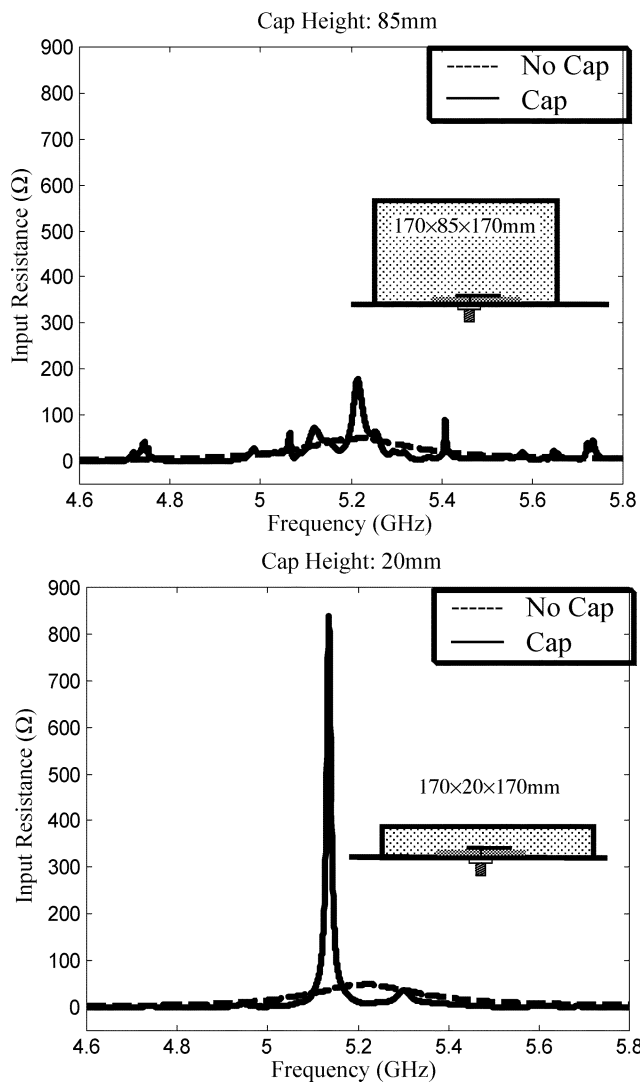
Fig. 3. Measured input resistance of a rectangular-shaped (17.5 mm × 24 mm) microstrip antenna built on Duroid before $(- - - - - -)$and after $(————)$applying the cap. (a) A Wheeler cap of size 170 mm × 85 mm × 170 mm. (b) A Wheeler cap of size 170 mm × 20 mm × 170 mm.
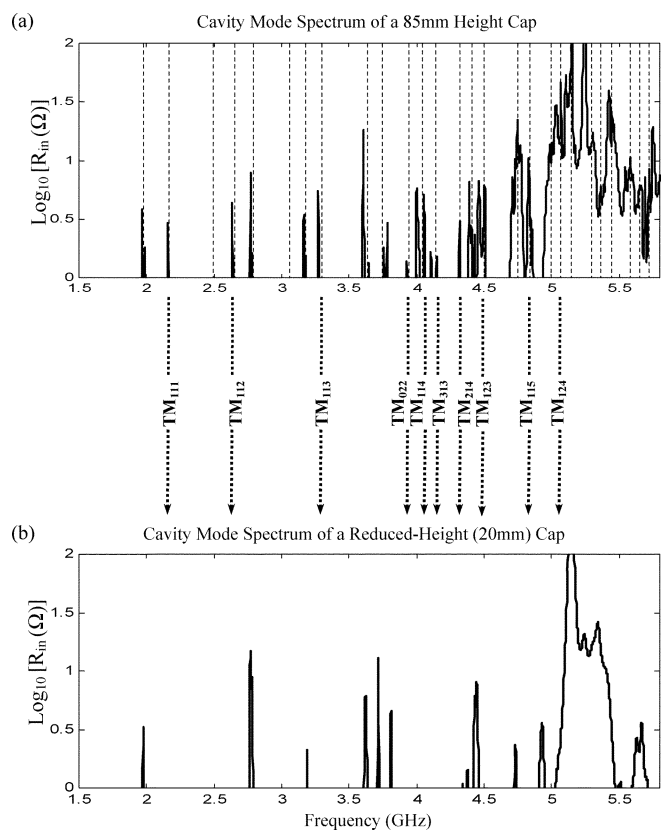


Fig. 4. Interior cavity mode spectra for two Wheeler cap sizes. (a) A Wheeler cap size of 170 mm × 85 mm × 170 mm. (b) A Wheeler cap size of 170 mm × 20 mm × × 170 mm.

resistance correspond closely to the permissible cavity modes predicted by (3).

By reducing the height of the Wheeler cap [dimension $b$ in (3)], it is possible to push the interior modes with index $N$ to higher frequencies, resulting in a much sparser mode spectrum. This idea is shown in Fig. 4(b). We see that the mode spectrum of the 20 mm height Wheeler cap is much sparser than that of the 85 mm one. In particular, the $N = 1$ and $N = 2$ modes have all disappeared from the lower frequency ranges as labeled between 4(a) and (b). (As the mode spectrum gets denser at higher frequencies, such identification becomes more difficult.) Sparser mode spectrum provides more frequency space in which to make the Wheeler cap measurement. We put this idea to test by measuring the input resistance of the same microstrip antenna shown in Fig. 3(a) using the reduced-height cap. The results, shown in Fig. 3(b), indeed show the sparser cavity mode spectrum we expected and a much more prominent microstrip patch resonance. Note that the resonant frequency of the microstrip antenna with cap is about 91 MHz lower than that without the cap due to the presence of the remaining cavity modes. As was done in [13], we adjust for this frequency shift in the data to match the resonant frequencies of the two measurements. After the frequency compensation, we obtain an efficiency value of 94% with this

reduced-height cap, which is closer to the gain simulation value of 99% than the efficiency of 73% by using the 85 mm cap. This shows that reduced-height Wheeler caps are helpful in obtaining a more accurate efficiency value while maintaining the length and width needed to enclose the microstrip antenna structure.

## IV. EFFICIENCY OF MINIATURIZED MICROSTRIP ANTENNAS

In this section, we apply the Wheeler cap method described above to measure the efficiency of miniaturized microstrip antennas designed using genetic algorithms [10]. [The photo of a typical GA antenna is shown in the inset of Fig. 5(a).] Our previous results showed that by using GA-optimized shapes, both the width and length of the patch could be reduced to 42% of the standard half-wavelength microstrip antenna while maintaining 65% of the original bandwidth. However, the efficiencies of these microstrip antennas are expected to degrade as a function of the degree of miniaturization. Fig. 5(a) and (b) show the efficiencies of the GA-designed microstrip antennas on FR-4 and Duroid substrate, respectively. The Wheeler cap measurements are shown as squares and the efficiencies obtained by the gain simulation are shown as X's. The simulated and measured efficiencies are in reasonable agreement. As expected, microstrip antennas built on high-loss FR-4 substrate have very low efficiency, even for a standard size patch (less than 35%). For miniaturized designs, the efficiency falls below 10%. The efficiencies on Duroid substrate are more reasonable. Even for the miniaturized designs, an efficiency of more than 65% can be maintained. However, this increase in efficiency is not without a tradeoff, as the achievable bandwidth using Duroid substrate is reduced compared to that using the FR-4 substrate.
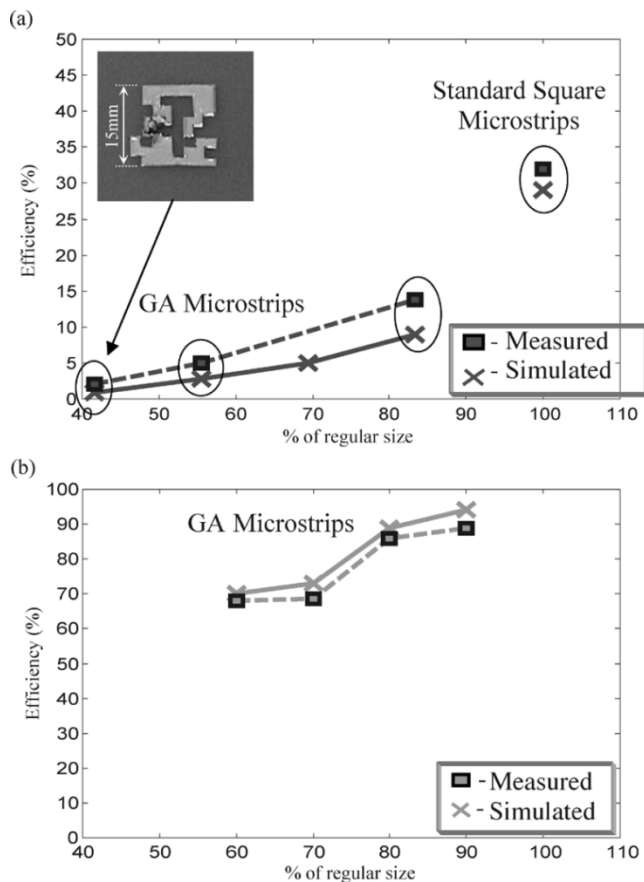
Fig. 5. (a) Efficiency of GA-designed microstrip antennas built on FR-4 substrate versus patch size (length or width as a percentage of the standard half-wavelength microstrip patch). (b) Efficiency of GA-designed microstrip patches built on Duroid.

## V. CONCLUSION

In this communication, we revisited the Wheeler cap method for measuring microstrip antenna efficiency and showed that the parallel *RLC* model is more appropriate for a single-resonance, probe-fed microstrip antenna on a thin substrate. The measured efficiency values were verified numerically using both the Wheeler cap and gain simulations. The observed agreements between the measurement and the simulations held over the entire −10 dB bandwidth around the antenna resonance. We also investigated interior cavity modes and found a way to alleviate their effects by using a reduced-height Wheeler cap. Finally, we applied the Wheeler cap method to measure the efficiency of miniaturized microstrip antennas designed by genetic algorithms on various substrate materials. The findings reported here are limited to the case of a single-resonance, probe-fed microstrip antenna on a thin substrate and may not be applicable for other cases.

## REFERENCES

[1] H. A. Wheeler, "The radiansphere around a small antenna," in *Proc. IRE*, Aug. 1959, pp. 1325–1331.
[2] E. Newman, P. Hohley, and C. H. Walter, "Two methods for the measurement of antenna efficiency," *IEEE Trans. Antennas Propag.*, vol. 23, no. 4, pp. 457–461, Jul. 1975.
[3] G. S. Smith, "An analysis of the Wheeler method for measuring the radiation efficiency of antennas," *IEEE Trans. Antennas Propag.*, vol. 25, no. 4, pp. 552–556, Jul. 1977.
[4] W. E. McKinzie, "A modified Wheeler cap method for measuring antenna efficiency," in *IEEE Antennas Propagat. Soc. Int. Symp. Dig.*, vol. 1, Jul. 1997, pp. 542–545.
[5] D. M. Pozar and B. Kaufman, "Comparison of three methods for the measurement of printed antenna efficiency," *IEEE Trans. Antennas Propag.*, vol. 36, no. 1, pp. 136–139, Jan. 1988.
[6] D. Pozar and D. H. Schaubert, *Microstrip Antennas*. New York: The Institute of Electrical and Electronics Engineers, 1995.
[7] J. R. James and P. S. Hall, *Handbook of Microstrip Antennas*. London, U.K.: Peter Peregrinus, 1989.
[8] K. R. Carver and J. W. Mink, "Microstrip antenna technology," *IEEE Trans. Antennas Propagat*, vol. 29, no. 1, pp. 2–24, Jan. 1981.
[9] R. Chair, K. M. Luk, and K. F. Lee, "Radiation efficiency analysis on small antenna by Wheeler cap method," *Microwave Optical Tech. Lett.*, vol. 33, pp. 112–113, Apr. 2002.
[10] H. Choo and H. Ling, "Design of broad-band and dual-band microstrip antennas on high-dielectric substrate using the genetic algorithm," *Proc. Inst. Elect. Eng.—Microwaves, Antennas Propagat.*, vol. 150, pp. 137–142, Jun. 2003.
[11] ENSEMBLE Version 8.0, Ansoft Corporation, Pittsburgh, PA.
[12] C. A. Balanis, *Advanced Engineering Electromagnetics*. New York: Wiley, 1989.
[13] R. L. Rogers, D. P. Buhl, H. Choo, and H. Ling, "Size reduction of a folded conical helix antenna," in *IEEE Antennas Propagat. Soc. Int. Symp. Dig.*, vol. 1, Jun. 2002, pp. 34–37.

# Effects of Antenna Element Bandwidth on Adaptive Array Performance

Inder J. Gupta, Jonathan A. Ulrey, and Edward H. Newman

*Abstract*—**The effects of individual antenna element bandwidth on the performance of adaptive arrays is studied when the incident interfering signals are wide-band signals. For these signal scenarios, as expected, the antenna element response over the bandwidth of the system plays an important role. If the individual antenna elements are dispersive, then the mutual coupling between array elements leads to dissimilar and dispersive channels in an adaptive array. This in turn leads to degradation in the performance of the adaptive array in that the adaptive array has to use more degrees of freedom to null a strong wide-band interfering signal. It is shown that by using wide-band antenna elements, one can significantly improve the performance of an adaptive array.**

*Index Terms*—**Adaptive antennas, element pattern, wide-band interference.**

## I. INTRODUCTION

It is well known that the radiation patterns of the individual elements, as well as the antenna geometry, affect the performance of an adaptive antenna array [1]–[6]. In the open literature, these effects have been studied for single tone [continuous wave (CW)] interfering signals. In the real world, the interfering signals incident on an antenna array are hardly single tones. Depending on the environment, the interfering signals can have the same bandwidth as the desired signals. Under these conditions, the response of the individual antenna elements over the system bandwidth would effect the adaptive antenna performance. In general, individual antenna elements are dispersive, i.e., the phase of